Dynamical Quantum Phase Transitions: Role of Topological Nodes in Wave Function Overlaps

Zhoushen Huang and Alexander V. Balatsky

Phys. Rev. Lett. **117**, 086802 — Published 15 August 2016

DOI: 10.1103/PhysRevLett.117.086802

Dynamical quantum phase transitions: Role of topological nodes in wavefunction overlaps

Zhoushen Huang[1] and Alexander V. Balatsky[1, 2]

[1] Institute for Materials Science, Los Alamos National Laboratory, Los Alamos, NM 87545, USA*
[2] NORDITA, Roslagstullsbacken 23, SE-106 91 Stockholm, Sweden†

A sudden quantum quench of a Bloch band from one topological phase toward another has been shown to exhibit an intimate connection with the notion of a dynamical quantum phase transition (DQPT), where the returning probability of the quenched state to the initial state—i.e. the Loschmidt echo—vanishes at critical times $\{t^*\}$. Analytical results so far are limited to two-band models, leaving the exact relation between topology and DQPT unclear. In this work, we show that for a general multi-band system, a robust DQPT relies on the existence of nodes (i.e. zeros) in the wavefunction overlap between the initial band and the post-quench energy eigenstates. These nodes are topologically protected if the two participating wavefunctions have distinctive topological indices. We demonstrate these ideas in detail for both one and two spatial dimensions using a three-band generalized Hofstadter model. We also discuss possible experimental observations.

Introduction Advances in experimental techniques, in particular in cold atom systems [1–3], have reinvigorated recent interest in quantum dynamics [4]. A paradigmatic setup in this context is a quantum quench [5–9], wherein a system is prepared as an eigenstate $|\Psi\rangle$ of an initial Hamiltonian H_I, but evolved under a different Hamiltonian H_F. In a slow ramp [10, 11], one has in addition the control over how fast the switching between H_I and H_F can be, as well as what path to take in the space of Hamiltonians. Since $|\Psi\rangle$ typically consists of many excited states of H_F with a non-thermal distribution, its time evolution provides a unique venue for investigating issues in nonequilibrium quantum statistical mechanics such as thermalization, equilibration, or the lack thereof [4, 12–16]. A particularly fruitful approach to understanding dynamics after a quantum quench is by exploiting the formal similarity between the time evolution operator $\exp(-iHt)$, and the thermal density operator $\exp(-\beta H)$. This enables one to leverage and extend notions in equilibrium statistical mechanics to the realm of quantum dynamics. In this spirit, the return amplitude

$$G(t) = \langle\Psi|e^{-iH_F t}|\Psi\rangle = \sum_n \left|\langle\Phi^{(n)}|\Psi\rangle\right|^2 e^{-iE_n t} \qquad (1)$$

can be thought of as a partition function along imaginary temperature $\beta = it$, with the prepared state $|\Psi\rangle$ as a fixed boundary [17]. Here $|\Phi^{(n)}\rangle$ and E_n are eigenstates and eigenvalues of the post-quench H_F, respectively. Heyl *et al* showed [18] that analogous to the thermal free energy, a dynamical free energy density [19] can be defined, $f(t) = -\log G(t)/L$, where L is system size. Singularities in f then signifies the onset of what was proposed as a *dynamical quantum phase transition* (DQPT). In statistical mechanics, phase transitions are closely related to the zeros of the partition function—known as Fisher zeros—in the complex temperature plane [20]. Historically, Yang and Lee were the first to connect phase transitions with zeros of the partition function in complexified parameter space [21]. While Fisher zeros are always complex for finite systems, they may coalesce into a continuum (line in one parameter dimension, area in two parameter dimensions, etc) that cuts through the real temperature axis in the thermodynamic limit, giving rise to an equilibrium phase transition. Investigations on DQPT have followed a similar route by first solving the Fisher zeros in the complex temperature plane, and then identifying conditions for them to cross the axis of imaginary temperature (real time). DQPT is thus mathematically identified as $G(t^*) = 0$ at critical time(s) t^* [22]. DQPTs occur in both integrable [18, 23–30] and non-integrable [19, 31–34] spin systems for quenches across quantum critical points. They can further be classified by discontinuities in different orders of time derivatives of $f(t)$ [27, 35] *vis-a-vis* their thermal counterparts. Very recently DQPTs have also been shown to constitute *unstable* fixed points in the renormalization group flow, and are therefore subject to the notion of universality class and scaling [36].

Physically, the return amplitude $G(t)$ is related to the power spectrum of work performed during a quench, $G(\omega) = \sum_n \left|\langle\Phi^{(n)}|\Psi\rangle\right|^2 \delta(\omega - (E_n - E_I))$, which is the Fourier transform of $G(t)e^{-iE_I t}$, and E_I is the energy of the initial state [37–40]. This in principle makes $G(t)$, and hence DQPT, a measurable phenomenon. A pratically more viable route to experimental verification is through measuring time evolution of thermodynamic quantities, which may exhibit post-quench oscillations at a time scale commensurate with the DQPT critical time t^*, and universal scaling near t^* [41]. In band systems, as we will show, they may also be identified by a complete depletion at t^* of sublattice or spin-polarized particle density at certain crystal momenta, see Eq. 8.

Parallel to the development of DQPT as the dynamical analogue of equilibrium phase transitions is the investigation on its relation with topology [24–27]. This issue arises naturally because in the transverse field Ising model, in which DQPT was first discovered, the quantum critical point can be mapped to a topological phase transition at which the quantized Berry phase of the *fermionized* Hamiltonian jumps between 0 and π. DQPT in this two-band fermion model was attributed to the occurrence of "population inversion" [18] where it becomes equally probable to find the initial state in either of the two post-quench bands, a consequence of the Berry phase jump [26]. The same analysis has been extended to various two-band models in one- and two-spatial dimensions (1D/2D) [25–29], where definitive connection was found between DQPT and quench across topological transitions, although some complications exist [42]. DQPTs have also been demonstrated to occur for quenches within the same topological phase [24, 25, 33], although from the point of view of topological protection, these are not robust as they require fine-tuning of the Hamiltonians.

The purpose of this work is to develop a general theory *beyond two band models* to clarify the relation between *robust* DQPT and topology. We will show that a robust DQPT—one which is insensitive to the details of the pre- and post-quench Hamiltonians other than the phases to which they belong—relies on the existence of zeros (or nodes) in the wavefunction overlap between the initial band and all eigenstates of the post-quench Hamiltonian. These nodes are topologically protected if the two participating wavefunctions have distinctive topological indices: for example, the Chern number difference $|C_\psi - C_\phi|$ provides a lower bound to the number of $\boldsymbol{k}$-space nodes in the overlap $\langle\phi_{\boldsymbol{k}}|\psi_{\boldsymbol{k}}\rangle$, see Theorem 1. These considerations lead to the notion of *topological* and *symmetry-protected DQPTs* which we will demonstrate in detail using a 3-band generalized Hofstadter model. Analysis of a 1D 3-band model exhibiting symmetry-protected DQPT can be found in Supplemental Materials (SM).

Amplitude and phase conditions of DQPT The DQPT condition $G(t^*) = 0$ can be interpreted geometrically as the complex numbers $z_n(t) = \left|\langle\Phi^{(n)}|\Psi\rangle\right|^2 e^{-iE_n t}$ forming a closed polygon in the complex plane at t^*, see Fig. 1. The time-independent content of this observation is that the amplitudes $\{|z_n|\}$ satisfy a generalized triangle inequality, $\sum_{m\neq n}|z_m| \geq |z_n|\ \forall n$. Invoking $\langle\Psi|\Psi\rangle = \sum_n |z_n| = 1$, one has the *amplitude condition*,

$$|z_n| = \left|\langle\Phi^{(n)}|\Psi\rangle\right|^2 \overset{!}{\leq} \frac{1}{2} \quad \forall n\ . \tag{2}$$

For $\{|z_n|\}$ that satisfy Eq. 2, solutions to $\sum_n |z_n| e^{-i\varphi_n} = 0$ exist and form a subspace $\mathcal{M}_{\{|z_n|\}}$ on the N-torus,

$$\mathcal{M}_{\{|z_n|\}} \in \mathcal{T}^N : \left\{ \{e^{-i\varphi_n}\} \middle| \sum_{n=1}^{N} |z_n| e^{-i\varphi_n} = 0 \right\}\ . \tag{3}$$

To set off DQPT, the dynamical phases must be able to evolve into $\mathcal{M}_{\{|z_n|\}}$. This constitutes the *phase condition*,

$$\exists t^* : \{e^{-iE_n t^*}\} \in \mathcal{M}_{\{|z_n|\}}\ . \tag{4}$$

DQPT requires both conditions to hold simultaneously.

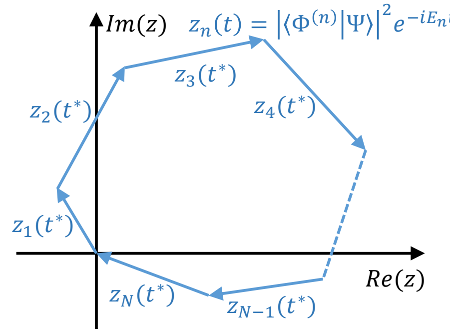

FIG. 1. (Color online) Geometric representation of the DQPT condition $G(t^*) = \sum_n z_n(t^*) = 0$. $\{z_n(t^*)\}$ must form a closed polygon in the complex plane, and hence satisfy a generalized triangle inequality $|z_n| \leq \sum_{m\neq n}|z_m|$. Wavefunction normalization $\langle\Psi|\Psi\rangle = \sum_n |z_n| = 1$ then leads to $|z_n| \leq \frac{1}{2}$

Phase ergodicity in few-level systems At first glance, the phase condition may seem to be the more stringent one. After a quench across a quantum phase transition, a many-body initial state $|\Psi\rangle$ typically has overlap with an extensive amount of eigenstates of the post-quench Hamiltonian H_F and therefore the amplitudes $\langle\Phi^{(n)}|\Psi\rangle$ are generically exponentially small in system size, rendering Eq. 2 satisfied in general. Existence of DQPT then relies entirely on the phase condition. Integrable systems, however, point to the possibility that the amplitude and phase conditions may be intricately related and traded for one another. Such systems can effectively be broken down into few-level subsystems labeled by quantum numbers $\boldsymbol{k}$, say $N_{\boldsymbol{k}}$ levels $\{E_{\boldsymbol{k},n}\}$ for $n = 1, 2, \cdots, N_{\boldsymbol{k}}$ in the $\boldsymbol{k}$ sector. Correspondingly $G(t) = \prod_{\boldsymbol{k}} G(\boldsymbol{k}, t)$. For the transverse field Ising model, Kitaev's honeycomb model [43], and band insulator models, $\boldsymbol{k}$ is the Bloch momentum. It is known that as long as the $N_{\boldsymbol{k}} - 1$ gaps, $\Delta_{\boldsymbol{k},n} = E_{\boldsymbol{k},n+1} - E_{\boldsymbol{k},n}$, are not rationally related, the dynamical phases $\{e^{-iE_{\boldsymbol{k},n}t}\}$ are *ergodic* on the $N_{\boldsymbol{k}}$-torus up to an overall phase [44], and *will* therefore evolve into its subspace $\mathcal{M}_{\{|z_n|\}}$ (Eq. 3). Phase ergodicity thus guarantees the phase condition Eq. 4, and DQPT in each $\boldsymbol{k}$ sector depends entirely on the amplitude condition.

Robust DQPT protected by nodes in wavefunction overlap Hereafter, we focus on quenches in multi-band Bloch systems with N_B bands. For simplicity we use a single filled band $|\psi(\boldsymbol{k})\rangle$ as the pre-quench state. Generalization to multiple filled bands is straightforward. The post-quench return amplitude is $G(t) = \prod_{\boldsymbol{k}} G(\boldsymbol{k}, t)$,

$$G(\boldsymbol{k}, t) = \sum_{n=1}^{N_B} \left|\langle\phi^{(n)}(\boldsymbol{k})|\psi(\boldsymbol{k})\rangle\right|^2 e^{-i\varepsilon_n(\boldsymbol{k})t}\ , \tag{5}$$

where $|\phi^{(n)}(\boldsymbol{k})\rangle$ and $\varepsilon_n(\boldsymbol{k})$ are respectively the post-quench energy eigenstates and eigenvalues. *Assume phase ergodicity holds at all* $\boldsymbol{k}$ *points*—this is a very relaxed requirement provided there is no degeneracy at any

$\boldsymbol{k}$ point. Then DQPT amounts to the existence of at least one $\boldsymbol{k}$ at which Eq. 2 is satisfied, namely

$$\exists \boldsymbol{k} \in \text{Brillouin Zone} : \left| \langle \phi^{(n)}(\boldsymbol{k}) | \psi(\boldsymbol{k}) \rangle \right|^2 \leq \frac{1}{2} \, \forall n \ . \quad (6)$$

We now discuss how Eq. 6 and hence DQPT can arise from nodes in wavefunction overlaps. Note that this is *not* the only way to get DQPT. Its virtue lies in its robustness against perturbations to the Hamiltonians. In SM, we provide examples where DQPTs with no overlap node can be easily avoided simply by Hamiltonian parameter tuning without crossing a phase boundary. The overlap nodes are, on the other hand, typically topologically protected, a point we will return to later. Now consider the following quench. Let $a = 1, 2, \cdots, N_B$ label "sublattices", which in general may also include other degrees of freedom, e.g., orbitals, spins, etc. Prepare the pre-quench state by filling $a = 1$,

$$|\Psi\rangle = \prod_{\boldsymbol{r}} \psi^\dagger_{\boldsymbol{r},1} |\emptyset\rangle = \prod_{\boldsymbol{k}} \psi^\dagger_{\boldsymbol{k},1} |\emptyset\rangle \ , \quad (7)$$

where $\psi^\dagger_{\boldsymbol{r},a}$ creates an electron on sublattice a in unit cell $\boldsymbol{r}$, $|\emptyset\rangle$ is the vacuum, $\psi^\dagger_{\boldsymbol{k},a} = \frac{1}{\sqrt{N}} \sum_{\boldsymbol{r}} e^{i\boldsymbol{k}\cdot\boldsymbol{r}} \psi^\dagger_{\boldsymbol{r},a}$, and N is the total number of unit cells. The system is then time-evolved under an integer quantum Hall Hamiltonian $\hat{H} = \sum_{\boldsymbol{k}} \hat{H}(\boldsymbol{k})$ where $\hat{H}(\boldsymbol{k}) = \sum_{a,b=1}^{N_B} H_{a,b}(\boldsymbol{k}) \psi^\dagger_{\boldsymbol{k},a} \psi_{\boldsymbol{k},b} = \sum_{n=1}^{N_B} \varepsilon_{\boldsymbol{k},n} \phi^\dagger_{\boldsymbol{k},n} \phi_{\boldsymbol{k},n}$, and we assume the Chern number of all bands of $\hat{H}(\boldsymbol{k})$ are non-zero, $C_n \neq 0 \, \forall n$. The overlap in Eq. 6 is $\langle \emptyset | \phi_{\boldsymbol{k},n} \psi^\dagger_{\boldsymbol{k},1} | \emptyset \rangle = \phi_1^{(n)}(\boldsymbol{k})^*$, where $\phi_a^{(n)}(\boldsymbol{k}) = \langle a | \phi^{(n)}(\boldsymbol{k}) \rangle$ is the a^{th} component of $|\phi^{(n)}(\boldsymbol{k})\rangle = (\phi_1^{(n)}(\boldsymbol{k}), \phi_2^{(n)}(\boldsymbol{k}), \cdots, \phi_{N_B}^{(n)}(\boldsymbol{k}))^t$, an eigenvector of the post-quench Hamiltonian matrix $H(\boldsymbol{k})$. It is known that any component $\phi_a^{(n)}(\boldsymbol{k}) \, \forall a$ must have *at least* $|C_n|$ zeros in the Brillouin zone [45], see also Thm. 1. Now assume at an arbitrary Bloch momentum $\boldsymbol{k}_0$, $\phi_1^{(n_1)}$ has the highest weight: $|\phi_1^{(n_1)}(\boldsymbol{k}_0)| > |\phi_1^{(n \neq n_1)}(\boldsymbol{k}_0)|$. The existence of node means $\phi_1^{(n_1)}$ cannot remain as the highest weight element over the entire Brillouin zone, and hence must switch rank with the second highest weight element, say $\phi_1^{(n_2)}$, at some point $\boldsymbol{k}_c$: $|\phi_1^{(n_1)}(\boldsymbol{k}_c)| = |\phi_1^{(n_2)}(\boldsymbol{k}_c)| \geq |\phi_1^{(n \neq n_1, n_2)}(\boldsymbol{k}_c)|$ [46]. Together with the normalization $\langle \emptyset | \psi^\dagger_{\boldsymbol{k},1} \psi_{\boldsymbol{k},1} | \emptyset \rangle = \sum_n |\phi_1^{(n)}|^2 = 1$, one concludes that at $\boldsymbol{k} = \boldsymbol{k}_c$, Eq. 6 is satisfied.

Note that in this case, the return amplitude $G(\boldsymbol{k}, t)$ is related to the $\boldsymbol{k}$-space sublattice particle density,

$$\rho_{\boldsymbol{k},a}(t) \equiv \langle \Psi(t) | \psi^\dagger_{\boldsymbol{k},a} \psi_{\boldsymbol{k},a} | \Psi(t) \rangle = |G(\boldsymbol{k}, t)|^2 \ . \quad (8)$$

A DQPT can thus be identified by $\rho_{\boldsymbol{k},a}(t^*) = 0$, i.e., a complete depletion of particles with momentum $\boldsymbol{k}$ on sublattice a (or orbital, spin, etc.), which may be experimentally measurable.

The argument above for node-protected DQPT applies to any pre-/post-quench combinations. In general, if the overlap of the pre-quench band $|\psi(\boldsymbol{k})\rangle$ with *every* eigenstate $|\phi^{(n)}(\boldsymbol{k})\rangle$ of $H_F(\boldsymbol{k})$ has nodes in the Brillouin zone, then the triangle inequality Eq. 6 is guaranteed, and a robust DQPT would occur. This criterion can be written in a form more amenable to numerical test,

$$\psi_{\mathsf{MaxMin}} \equiv \max_n \left[\min_{\boldsymbol{k}} \left| \langle \phi^{(n)}(\boldsymbol{k}) | \psi(\boldsymbol{k}) \rangle \right| \right] \ , \quad (9)$$

$$\psi_{\mathsf{MaxMin}} = 0 \Leftrightarrow \text{Robust DQPT} \ . \quad (10)$$

Topological protection of nodes in wavefunction overlaps There is a curious connection between wavefunction zeros and quantization. In elementary quantum mechanics, nodes in the radial wavefunction is related to the principal quantum number [47]. In continuum integer quantum Hall systems, the number of nodes in the wavefunction $\psi(\boldsymbol{r}) = \langle \boldsymbol{r} | \psi \rangle$ for $\boldsymbol{r}$ in a magnetic unit cell is given by its Chern number magnitude $|C|$ [45]. These nodes persist even in the presence of weak disorder [48]. On a lattice, $|C|$ gives the number of $\boldsymbol{k}$-space nodes in all wavefunction components $\psi_a(\boldsymbol{k}) = \langle a | \psi(\boldsymbol{k}) \rangle \forall a$ [45], a phenomenon closely related to the energetic spectral flow of the edge states [49]. Note that the relation between C and wavefunction nodes relies on one participant of the overlap, namely the basis states $|\boldsymbol{r}\rangle$ and $|a\rangle$, to be topologically trivial. If both participants can be nontrivial, the number of nodes in their overlap should depend on both topological indices on an equal footing. Indeed we have the following theorems,

Theorem 1 *In 2D, the overlap of Bloch bands $|\psi(\boldsymbol{k})\rangle$ and $|\phi(\boldsymbol{k})\rangle$, with Chern numbers C_ψ and C_ϕ respectively, must have at least $|C_\psi - C_\phi|$ nodes in the Brillouin zone.*

Theorem 2 *In 1D, the Berry phase γ of a real Bloch band, $|\psi(k)\rangle = (\psi_1(k), \psi_2(k), \cdots)^t, \psi_a(k) \in \mathbb{R} \forall a$, is quantized to 0 or π. The overlap of two real bands $|\psi(k)\rangle$ and $|\phi(k)\rangle$, with Berry phases γ_ψ and γ_ϕ respectively, must have at least one node if $\gamma_\psi \neq \gamma_\phi$.*

See SM for proof. Note that symmetry protection may enforce a Hamiltonian to be real [50], leading to the real bands in Thm. 2. This prompts the notion of *symmetry-protected DQPT*, reminiscent of symmetry-protected topological phases that may be classified by topological numbers at high-symmetry hyper-surfaces [50–52]. An example will be given later, see also SM.

Generalized Hofstadter model We demonstrate ideas discussed above using a generalized Hofstadter model,

$$H(\boldsymbol{k}, t, m) = \begin{pmatrix} d_1 & v_1 & v_3 e^{ik_y} \\ v_1 & d_2 & v_2 \\ v_3 e^{-ik_y} & v_2 & d_3 \end{pmatrix} \ , \quad (11)$$

$$d_a = 2\cos(k_x + a\varphi) + am \ ,$$

$$v_a = 1 + 2t \cos\left[k_x + (a + \frac{1}{2})\varphi \right] \ ,$$

$$a = 1, 2, 3 \ , \ \varphi = \frac{2\pi}{3} \ .$$

The nearest neighbor hopping is set as 1. At $t = m = 0$, we recover the Hofstadter model [49, 53–58] on a square lattice with magnetic flux φ per structural unit cell, and its magnetic unit cell consists of 3 structural unit cells along the y direction. $t \neq 0$ allows for second neighbor (i.e. diagonal) hopping, and $m \neq 0$ describes a flux-commensurate onsite sawtooth potential. See SM for phase diagram. At $k_y = 0$ and π, $H(\boldsymbol{k})$ is invariant under the combined transformation of time-reversal, $H(\boldsymbol{k}) \to H^*(-\boldsymbol{k})$, and inversion, $H(\boldsymbol{k}) \to H(-\boldsymbol{k})$, and is hence real. Eigenstates there are subject to Thm. 2.

Now consider quenches in which the initial state is prepared by filling one of the three bands of a pre-quench Hamiltonian parameterized by t_i, m_i, and evolved using a post-quench Hamiltonian with t_f, m_f [59]. In Fig. 2, we keep t_i, m_i, m_f fixed, and plot the MaxMin (Eq. 9) of the three pre-quench bands as functions of the post-quench t_f. By varying t_f, the post-quench $H(\boldsymbol{k})$ is swept through six different topological phases as labeled in Fig. 2.

Let us illustrate topological and symmetry-protected DQPTs with two examples, using $\psi^{(2)}$ as the pre-quench state (blue circled line in Fig. 2): (i) *Topological DQPT* protected by 2D Chern number. Consider the quench from $\psi^{(2)}$ to phase 5. In this case, the Chern number of the pre-quench state ($C = -1$) differs from *all* three Chern numbers of the post-quench Hamiltonian ($C = [1, -2, 1]$), thus from Thm. 1, all three overlaps have nodes, and Eq. 6 is satisfied. (ii) *Symmetry-protected DQPT*. Consider the quench from $\psi^{(2)}$ to phase 2. In this case, the pre-quench Chern number ($C = -1$) is identical to at least one of the post-quench Chern numbers ($C = [0, 1, -1]$), hence not all overlaps have nodes originating from Thm. 1. Nevertheless, at $k_y = 0$ and π where the Hamiltonian is real, its eigenstates can be classified by their Berry phases. One can find numerically that at $k_y = 0$, the Berry phase for $\psi^{(2)}$ is $\gamma = 0$, whereas that of the post-quench $\phi^{(3)}$ (the one with $C = -1$) is $\gamma = \pi$. According to Thm. 2, therefore, $\langle \phi^{(3)} | \psi^{(2)} \rangle_{k_y=0}(k_x)$ has node along k_x. Nodes in overlaps of $\psi^{(2)}$ with $\phi^{(1)}$ and $\phi^{(2)}$ are still protected by Thm. 1. Thus all three overlaps have nodes and DQPT is protected.

Details of all 18 quench types (3 pre-quench states × 6 post-quench phases) can be found in SM. We should note here that out of all 18 types, 2 robust DQPTs ($\psi^{(1)}$ to phases 2 and 5) exhibit an even number of overlap nodes at $k_y = 0$ and/or π not accounted for by Thms. 1 and 2. By tuning $t_{i,f}$ and $m_{i,f}$, we were able to shift the nodes along k_x as well as to change the total number of nodes by an even number, but could not entirely eliminate them. We suspect however that they could eventually be eliminated in an enlarged parameter space.

Conclusion and discussion In this work, we showed that for quantum quenches between gapped phases in a generic multi-band system, a robust dynamical quantum phase transition (DQPT) is a consequence of momentum-space nodes (or zeros) in the wavefunction overlap between the pre-quench state and all post-quench energy eigenstates. Nodes in wavefunction overlaps are topologically protected if the topological indices of the two participating wavefunctions—such as Chern number in 2D and Berry phase in 1D—are different.

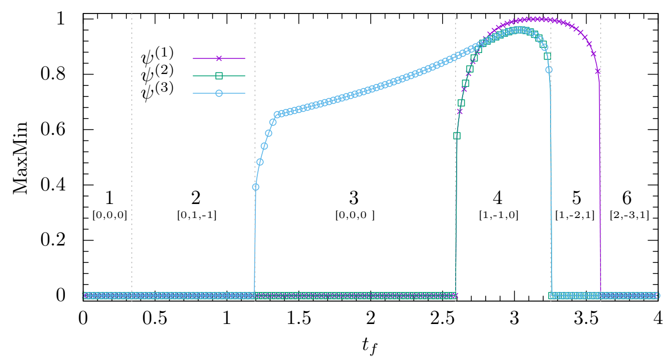

FIG. 2. (Color online) Plot of ψ_{MaxMin} (Eq. 9) as functions of the post-quench t. Pre-quench state is prepared by filling one of the three bands $\psi^{(1,2,3)}$ of the generalized Hofstadter model Eq. 11 with parameters $t_i = 3$ and $m_i = 2.8$. Post-quench $H(\boldsymbol{k})$ has fixed $m_f = 3$ and a varying t_f, sweeping it through six topological phases labeled by its three Chern numbers (ordered from lower to higher band). The pre-quench Hamiltonian is in phase 4. A robust DQPT can be identified by $\psi_{\mathsf{MaxMin}} = 0$ (Eq. 10). Note that ψ_{MaxMin} changes between zero and non-zero only at phase boundaries, verifying robust DQPT as a feature of topological phases insensitive to parameter tuning. See SM for detailed account of all 18 types of quenches shown here.

Our main tenets here are the triangle inequality Eq. 6, and phase ergodicity. It is interesting to note that collapsing a band gap would affect both conditions: right at the gap collapsing point $\varepsilon_{\boldsymbol{k}}^{(n)} = \varepsilon_{\boldsymbol{k}}^{(n+1)}$, the two phases become mutually locked; as the gap re-opens, the system has gone through a topological transition, which changes the node structure in wavefunction overlaps. We also note that while the *existence* of topological and symmetry-protected DQPT is insensitive to details of the energy band structure, the exact times at which it would occur will inevitably depend on the latter. The shortest critical time will be upper-bounded by the recurrence time of the phases, which, for few-level systems such as band insulators, should remain physically relevant [60].

DQPT in band systems is in principle experimentally measurable. As shown in Eq. 8, DQPT can be identified as the depletion of "sublattice" particle density $\rho_{\boldsymbol{k},a}(t^*)$ where sublattice a can also refer to spin, orbital, etc. Particle density $\rho_{\boldsymbol{k}}(t) = \sum_a \rho_{\boldsymbol{k},a}(t)$ can already be measured in cold atom systems by time-of-flight experiments [1–3, 54, 61]. It is not hard to envisage an additional procedure of "sublattice" isolation in such measurements, e.g., by using a magnetic field for spin filtering, or by releasing other sublattices $b \neq a$ slightly earlier than a.

Acknowledgments We are grateful to D.P. Arovas, A. Alexandradinata, and A. Saxena for useful discussions. We thank J.M. Zhang for communication of a recent work [62]. Work at LANL was supported by the US DOE BES E304/E3B7. Work at NORDITA was supported by ERC DM 321031.

* zsh@lanl.gov
† avb@nordita.org

[1] I. Bloch, J. Dalibard, and W. Zwerger, Rev. Mod. Phys. **80**, 885 (2008).
[2] I. Bloch, J. Dalibard, and S. Nascimbène, Nature Physics **8**, 267 (2012).
[3] T. Langen, R. Geiger, and J. Schmiedmayer, Annual Review of Condensed Matter Physics **6**, 201 (2015), 1408.6377.
[4] A. Polkovnikov, K. Sengupta, A. Silva, and M. Vengalattore, Rev. Mod. Phys. **83**, 863 (2011).
[5] F. Iglói and H. Rieger, Phys. Rev. Lett. **85**, 3233 (2000).
[6] E. Altman and A. Auerbach, Phys. Rev. Lett. **89**, 250404 (2002).
[7] A. Polkovnikov, S. Sachdev, and S. M. Girvin, Phys. Rev. A **66**, 053607 (2002).
[8] K. Sengupta, S. Powell, and S. Sachdev, Phys. Rev. A **69**, 053616 (2004).
[9] P. Calabrese and J. Cardy, Physical Review Letters **96**, 136801 (2006), cond-mat/0601225.
[10] R. Barankov and A. Polkovnikov, Physical Review Letters **101**, 076801 (2008), 0804.2894.
[11] F. Pollmann, S. Mukerjee, A. G. Green, and J. E. Moore, Phys. Rev. E **81**, 020101 (2010).
[12] R. Nandkishore and D. A. Huse, Annual Review of Condensed Matter Physics **6**, 15 (2015), 1404.0686.
[13] J. Eisert, M. Friesdorf, and C. Gogolin, Nature Physics **11**, 124 (2015), 1408.5148.
[14] L. D'Alessio, Y. Kafri, A. Polkovnikov, and M. Rigol, ArXiv e-prints (2015), 1509.06411.
[15] F. H. L. Essler and M. Fagotti, ArXiv e-prints (2016), 1603.06452.
[16] J. Millen and A. Xuereb, New Journal of Physics **18**, 011002 (2016), 1509.01086.
[17] A. LeClair, G. Mussardo, H. Saleur, and S. Skorik, Nuclear Physics B **453**, 581 (1995), hep-th/9503227.
[18] M. Heyl, A. Polkovnikov, and S. Kehrein, Phys. Rev. Lett. **110**, 135704 (2013).
[19] M. Fagotti, ArXiv e-prints (2013), 1308.0277.
[20] M. E. Fisher, *The Nature of Critical Points*, vol. 7 of *Lectures in Theoretical Physics* (the University of Colorado Press, 1965).
[21] C. N. Yang and T. D. Lee, Phys. Rev. **87**, 404 (1952). T. D. Lee and C. N. Yang, Physical Review **87**, 410 (1952).
[22] Note1, the formal similarity between e^{-iHt} and $e^{-\beta H}$ is routinely used in field theoretic calculations such as correlators, where the thermal and quantum-dynamic results are related through Wick rotation. Knowledge in one domain can then be transcribed into the other without additional calculation. This "equivalence", however, relies on the existence of an analytic continuation between it and β in the complex temperature plane. The presence of closed and/or semi-infinite Fisher zero lines divide the complex temperature plane into disjoint regions, and the correspondence between it and β will break down if they reside in different regions. For quenches that exhibit DQPT, as pointed out in Ref. [18], this implies that non-equilibrium time evolution (i.e. along the imaginary temperature axis) is in general not governed by the equilibrium thermodynamics (along the real temperature axis).
[23] B. Pozsgay, Journal of Statistical Mechanics: Theory and Experiment **10**, 10028 (2013), 1308.3087.
[24] S. Vajna and B. Dóra, Phys. Rev. B **89**, 161105 (2014).
[25] J. M. Hickey, S. Genway, and J. P. Garrahan, Phys. Rev. B **89**, 054301 (2014).
[26] S. Vajna and B. Dóra, Phys. Rev. B **91**, 155127 (2015).
[27] M. Schmitt and S. Kehrein, Phys. Rev. B **92**, 075114 (2015).
[28] U. Divakaran, S. Sharma, and A. Dutta, ArXiv e-prints (2016), 1601.04851.
[29] S. Sharma, U. Divakaran, A. Polkovnikov, and A. Dutta, ArXiv e-prints (2016), 1601.01637.
[30] J. C. Budich and M. Heyl, Phys. Rev. B **93**, 085416 (2016).
[31] C. Karrasch and D. Schuricht, Phys. Rev. B **87**, 195104 (2013).
[32] J. N. Kriel, C. Karrasch, and S. Kehrein, Phys. Rev. B **90**, 125106 (2014).
[33] F. Andraschko and J. Sirker, Phys. Rev. B **89**, 125120 (2014).
[34] S. Sharma, S. Suzuki, and A. Dutta, Phys. Rev. B **92**, 104306 (2015).
[35] E. Canovi, P. Werner, and M. Eckstein, Phys. Rev. Lett. **113**, 265702 (2014).
[36] M. Heyl, Phys. Rev. Lett. **115**, 140602 (2015).
[37] P. Talkner, E. Lutz, and P. Hänggi, Phys. Rev. E **75**, 050102 (2007), cond-mat/0703189.
[38] M. Campisi, P. Hänggi, and P. Talkner, Reviews of Modern Physics **83**, 771 (2011), 1012.2268.
[39] C. Jarzynski, Phys. Rev. Lett. **78**, 2690 (1997).
[40] S. Deffner and A. Saxena, Phys. Rev. E **92**, 032137 (2015).
[41] M. Heyl, Phys. Rev. Lett. **113**, 205701 (2014).
[42] Note2, e.g., in 2D integer quantum Hall systems, DQPT is related to the change in the *absolute value* of Chern number $|C|$ instead of C [26].
[43] A. Kitaev, Annals of Physics **321**, 2 (2006), cond-mat/0506438.
[44] I. Cornfeld, A. Sossinskii, S. Fomin, and Y. Sinai, *Ergodic Theory* (Springer, 1982).
[45] M. Kohmoto, Annals of Physics **160**, 343 (1985).
[46] Note3, for two band models, $\boldsymbol{k}_c$ is where the so-called "population inversion" occurs.
[47] L. D. Landau and E. M. Lifshits, *Quantum Mechanics: Non-relativistic Theory* (Butterworth-Heinemann, 1977).
[48] D. P. Arovas, R. N. Bhatt, F. D. M. Haldane, P. B. Littlewood, and R. Rammal, Phys. Rev. Lett. **60**, 619 (1988).
[49] Y. Hatsugai, Phys. Rev. Lett. **71**, 3697 (1993).
[50] C. Fang, Y. Chen, H.-Y. Kee, and L. Fu, Phys. Rev. B **92**, 081201 (2015), 1506.03449.
[51] S. Ryu, A. P. Schnyder, A. Furusaki, and A. W. W. Ludwig, New Journal of Physics **12**, 065010 (2010), 0912.2157.
[52] A. Alexandradinata, C. Fang, M. J. Gilbert, and B. A. Bernevig, Phys. Rev. Lett. **113**, 116403 (2014).
[53] D. R. Hofstadter, Phys. Rev. B **14**, 2239 (1976).

[54] E. Zhao, N. Bray-Ali, C. J. Williams, I. B. Spielman, and I. I. Satija, Phys. Rev. A **84**, 063629 (2011).

[55] Z. Huang and D. P. Arovas, Phys. Rev. B **86**, 245109 (2012), 1201.0733.

[56] L. Wang, A. A. Soluyanov, and M. Troyer, Physical Review Letters **110**, 166802 (2013), 1303.1061.

[57] F. Harper, S. H. Simon, and R. Roy, Phys. Rev. B **90**, 075104 (2014), 1404.5303.

[58] M. Aidelsburger, M. Lohse, C. Schweizer, M. Atala, J. T. Barreiro, S. Nascimbène, N. R. Cooper, I. Bloch, and N. Goldman, Nature Physics **11**, 162 (2015), 1407.4205.

[59] Note4, an initial state of two filled bands is equivalent to one with a single filled band through particle-hole transformation.

[60] Note5, under special circumstances, the DQPT critical time may also emerge at a much shorter time scale, e.g., the inverse level spacing, see Ref. [62].

[61] D.-L. Deng, S.-T. Wang, and L.-M. Duan, Phys. Rev. A **90**, 041601 (2014).

[62] J. M. Zhang and H.-T. Yang, ArXiv e-prints (2016), 1601.03569.